MIT Open Access Articles

Real-time transmission-type terahertz microscope with palm size terahertz camera and compact quantum cascade laser

Massachusetts Institute of Technology

Real-Time Transmission-type Terahertz Microscope, with

Palm size Terahertz Camera and Compact Quantum Cascade Laser

Naoki Oda[a1], Tsutomu Ishi[a], Takao Morimoto[a], Takayuki Sudou[a],

Hitoshi Tabata[b], Shunsuke Kawabe[b], Kyohei Fukuda[b],

Alan W. M. Lee[c,d] and Qing Hu[d]

[a] NEC Guidance and Electro-Optics Division
[b] Department of Bio-Engineering, The University of Tokyo
[c] LongWave Photonics LLC
[d] Massachusetts Institute of Technology

ABSTRACT

This paper describes a real-time transmission-type Terahertz (THz) microscope, with palm-size THz camera and compact quantum cascade laser (QCL). The THz camera contains 320x240 microbolometer focal plane array which operates at 30 Hz frame rate and has lock-in imaging function as well as integration functions such as frame integration and spatial filter. These functions are found very powerful in improving signal-to-noise ratio. QCL is installed in compact Stirling cycle cooler. A variety of QCLs covers frequency range from 1.5 to 5 THz and provides time-average power of 0.5~2 mW. The illumination area for sample is changed by adjusting one lens in the illumination optics. Performances of the THz microscope, such as signal-to-noise ratio and so on, were measured and are found consistent with the calculations. THz images taken with the THz microscope are finally presented.

Keywords : THz Microscope, Transmission-type, THz Camera, Quantum Cascade Laser

1. INTRODUCTION

Terahertz (THz) technology is very much expected to be applied to biomedical imaging[1],[2], non-destructive inspection[3], security[4],[5] and so forth, because biological macromolecules have spectral features in the THz frequency region, and THz radiation is transparent to papers, clothes, plastics, etc. Time Domain Spectroscopy (TDS) technique has been used in most of cases to investigate spectral features for a variety of materials and depth profiles of layered materials since early 2000[6],[7]. Along with spectroscopic systems, THz imaging techniques have also been developed,

―――――――――――――
1   Correspondence   Email: n-oda@cb.jp.nec.com   Phone:+81-42-333-1150;   Fax:+81-42-333-1888

using TDS with raster scanning of a sample[8]. However, this technique requires a long acquisition time to form an image, making the development of both real-time THz imager and strong THz radiation source desirable. This requirement can be achieved with a combination of palm-size and real-time THz imager with compact quantum cascade laser (QCL)[9]. According to the reference [9], the palm-size THz imager includes 320x240 microbolometer-type uncooled focal plane array (FPA) which operates at 30 Hz frame rate and has nearly flat spectral response over a frequency range from ca. 1.5 to 100 THz, and the QCL which is installed in compact closed-cycle cryocooler can cover a frequency range from ca. 1.5 to 5 THz.

From the viewpoint of atmospheric extinction, calculation based on HITRAN shows that high transmittance is obtained only for path length shorter than ca. 1 m in the frequency region higher than 1 THz, while below 1 THz high transmittance is obtained even for 10 m path length. Here, the calculations were carried out at 23 Celsius and 60% relative humidity. This calculation indicates that the combination of the palm-size THz imager with the compact QCL is suitable for applications of short standoff range, such as THz microscope for biomedical imaging and equipments for non-destructive process control.

This paper describes the transmission-type THz microscope, which consists of THz-QCL, illumination optics and THz camera. Design concept of the illumination optics is explained, and specifications and performances of both THz-QCL and THz camera are summarized. The performances of the THz microscope, such as signal-to-noise ratio and spatial resolution, are presented, and finally THz imageries are shown.

2. TRANSMISSION-TYPE THz MICROSCOPE

Figures 1 and 2 show a picture of transmission-type THz microscope and its layout, respectively. The microscope consists of THz radiation source, illumination optics and THz camera. Easy QCL (LongWave Photonics LLC) is used as THz radiation source. Frequency of emission line from QCL is 2.83 THz (wavelength 106 μm). Divergent beam from QCL is collected and focused with illumination optics, which is composed of seven high-resistivity Si lenses (L1-L7), a plane mirror (M1) and aperture. These Si lenses are coated on both sides with anti-reflection layers for 2.83 THz. The first lens (L1) is designed to convert any QCL beam to a beam with a cone angle of 30 degree. This beam is collected and focused at an aperture with the lenses (L2 and L3) and mirror (M1). The beam from the aperture illuminates sample through the lenses (L4 and L5). The size of the illumination area is adjustable by moving the lens (L5). Changing the aperture size may reduce influence of interference pattern resulting from strong coherency of QCL's line emission. The illumination area is observed with THz-FPA integrated in THz camera (IRV-T0831, NEC) through microscopic optics which consists of two lenses (L6 and L7) and infrared blocking filter (QMC Instruments, Ltd). The microscopic lens has a magnification ratio of 1, a numerical aperture of 0.5 and ca. 30 mm working distance between the lens and sample. The infrared blocking filter has both excellent features of infrared blocking and long pass transmission (see Fig.3). Table 1 summarizes the parameters of the transmission-type THz microscope.
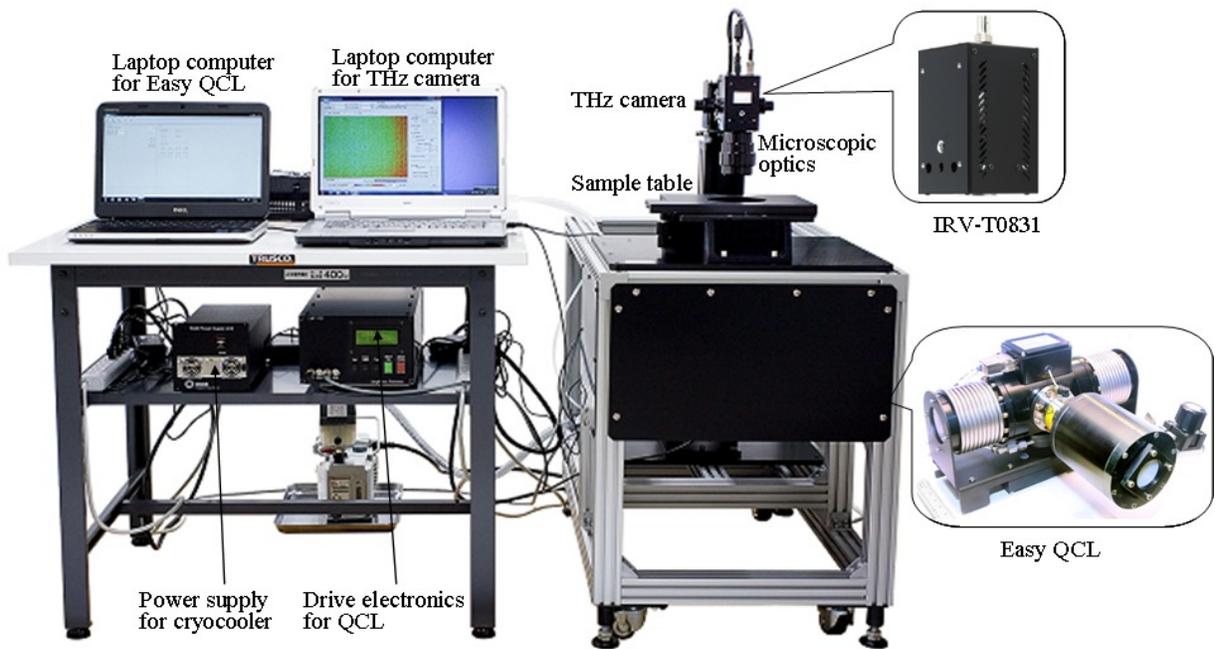
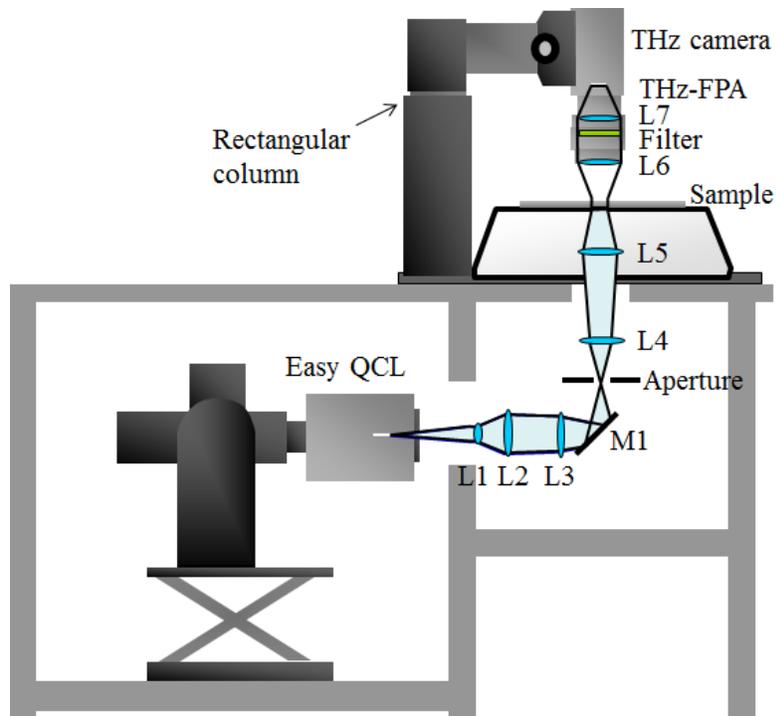Fig.1 A picture of transmission-type THz microscope

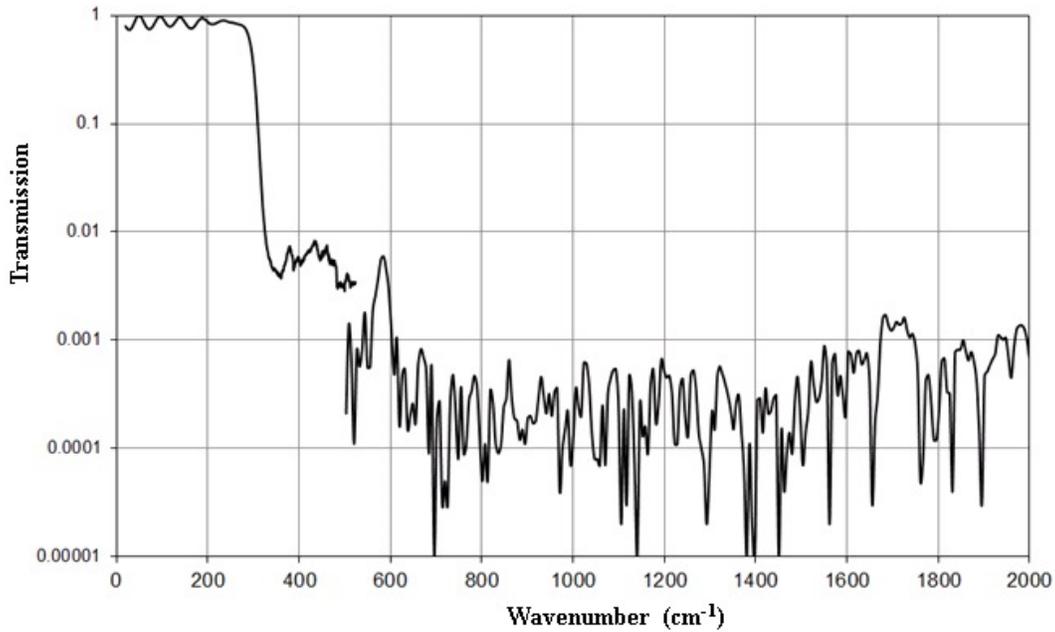Fig.2 A layout of transmission-type THz microscope

Fig.3 Transmission curve of the infrared blocking filter (QMC Instruments, Ltd)

Table 1 Parameters of transmission-type THz microscope

Components	Comments
THz radiation source	QCL[*]
THz illumination area	From ca. 2 to 10 mm in diameter[**]
THz camera	Microbolometer-type 320x240 THz-FPA (23.5 μm pitch) Frame rate : 30 Hz Integration functions : Frame integration, Spatial filter Lock-in imaging function
Magnification ratio of microscopic optics	1
Numerical aperture of microscopic optics	0.5
Infrared blocking filter (Long pass metal mesh filter)	Cut-on wavelength : ca. 30 μm
Working distance between sample and optics	ca. 30 mm
Others	Extra instruments, such as optical microscope, can be attached around rectangular column.

[*]) Frequency of emission line is selectable (see Fig.5)

[**]) The illumination area is adjustable by moving the lens L5.

2-1. EASY-TO-USE THz QUANTUM CASCADE LASER

Growth, fabrication, and characterization of QCLs are detailed in reference [10]. The QCL active region is fabricated into metal-metal waveguides with typical dimensions of 1 mm × 100 μm × 10 μm. This waveguide consists of a ground plane, on which the GaAs/AlGaAs active region is formed, and a top metal contact. This waveguide allows near unity optical mode overlap with the gain medium, leading to lower laser threshold-currents and higher operating temperature performance. However, this high confinement also results in high end-facet reflectivity of 70~90%, depending on wavelength and geometry. To increase the outcoupling (reduction in reflectivity), a silicon hyper-hemispherical lens is attached to the facet of the waveguide. This lens has two very desirable effects: increasing the output power by factors of ~5, and dramatically reducing the beam divergence to values < 30 deg. The packaged QCL is shown in Fig.4, which is mounted in the Stirling cycle cryocooler and is cooled at temperature of 50~60 K. Time-averaged output power levels of various QCLs are summarized in Fig.5. The time-average power is essential for microbolometer THz-FPA, because it usually has thermal time constant of 10 - 20 msec. Duty cycle of 2 % (pulse width: 200 nsec) is usually applied to pulsed operation, but larger value of duty cycle, such as 25% can be applied.

The QCL used in the microscope (2.83 THz) is usually operated at 60 K to make observation time longer, so that the typical time-averaged output power is ca. 0.54 mW (duty cycle 8 %). In a later section, signal-to-noise ratio (SNR) is discussed for illumination area without sample.
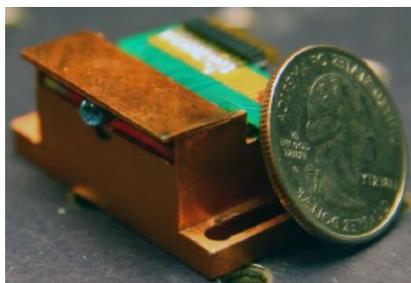

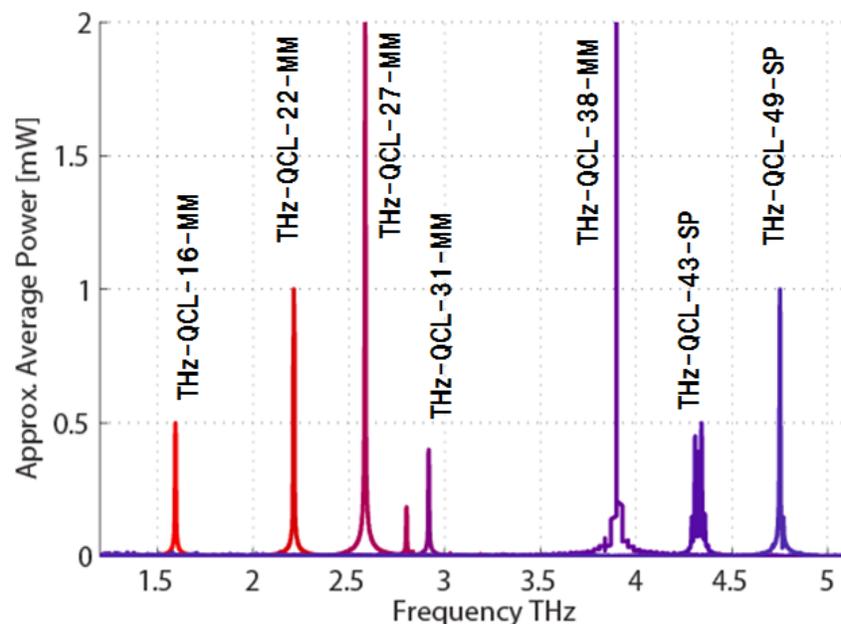Fig.4 Packaged QCL with

hyper-hemispherical lens

Fig.5 Frequency dependence of approximate time-average powers from QCLs

(operation temperature: ca. 50 K)

2-2. PALM-SIZE THz CAMERA

Palm-size uncooled THz camera (see Fig.6) was developed and its specifications are listed in table 2. The THz camera contains microbolometer-type THz-FPA with 320x240 array format and 23.5 μm pitch[11]. Wavelength dependence of NEP (Noise Equivalent Power) for THz-FPA itself is shown in Fig.7[9], where the solid curve is a calculated one, based on the formulae about absorptance of microbolometer structure [11]. In the calculations, absorptance and NEP are normalized at 70 μm. In wavelength range shorter than 70 μm, SiN (main material of microbolometer structure) starts to absorb radiation, so that the formulae probably do not work. The THz camera has a linear dynamic range of ca. 1000, which was obtained in combination of QCL with a set of attenuation filters.

The THz camera is controlled with a computer which has functions of signal processing, such as frame integration and spatial filter, to increase signal-to-noise ratio (SNR). However, the most powerful function of the camera is a lock-in imaging function to further increase SNR. One of outputs, sync signal can control switching THz radiation sources on/off, such as QCL, optical chopper and so forth. THz image taken in THz source-off phase is subtracted from THz image taken in THz source-on phase, so that SNR increases as a function of square root of the number of integrated frames. This is because 1/f noise is removed by the lock-in function.

Table 2. Specifications of palm-size THz camera (IRV-T0831)

Array format - pixel pitch	320 x 240 - 23.5 μm
Outputs	Digital image data : USB2.0 Sync signal (TTL level) : BNC
Frame rate	30Hz
Lock-in imaging function	Lock-in frequency 15, 7.5, 3.75 and 1.875 Hz
Weight	ca. 550g
Size	ca. 64mm^W x 62mm^H x 103mm^D

Fig.6 Palm-size THz camera
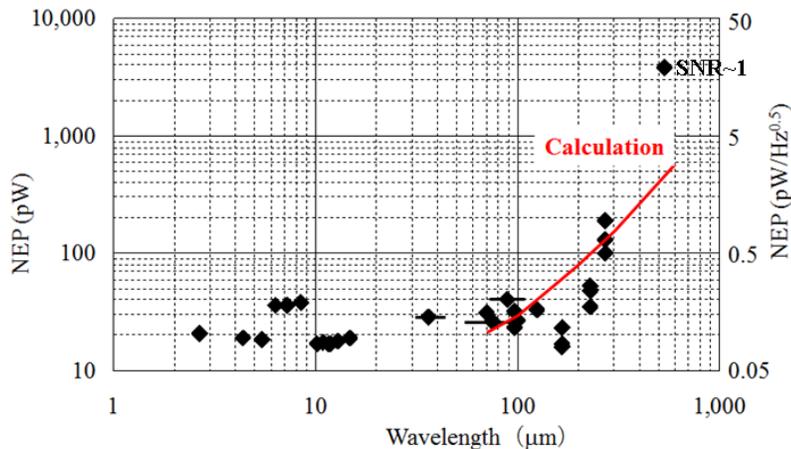

Fig.7 Wavelength dependence of NEP for THz-FPA itself (Data point at 550 μm has SNR of ca. 1)

2-3. OVERALL PERFORMANCE OF THz MICROSCOPE

First of all, the amount of incident QCL power per pixel is estimated and is compared with the amount of incident background radiation (300K blackbody) per pixel. As to the latter, two different wavelength regions are considered, namely, wavelength region longer than 30 μm and wavelength region shorter than 30 μm.

In estimating the amount of incident QCL power per pixel, illumination area of 5.64 mm in diameter is taken, which corresponds to 240 pixels in THz-FPA. Transmission curve of 1 mm thick Si disk coated on both sides with anti-reflection layers for 2.83 THz was measured and its transmittance is found 94 % at 2.83 THz. Since seven Si lenses exist between QCL and THz-FPA, and the thickest parts of seven Si lenses have 23.4 mm thickness in total, the absorptance of the remaining 16.4 mm thick part is estimated to be 72 %, using absorption coefficient of 0.2 cm^{-1}[11]. Atmospheric transmittance is also calculated to be 61 % for conditions of 24 Celsius, 58 % relative humidity and 64 cm distance between QCL and THz-FPA. Thus, the incident QCL power is calculated to be ca. 3 nW/pixel.

In estimating the amount of incident 300K background radiation around sample, two lenses (L6 and L7), filter and Si package window are considered. In THz region (wavelength longer than 30 μm), the incident 300K background radiation is calculated to be ca. 1 nW/pixel. Thanks to the excellent infrared blocking feature of the filter (Fig.3), the amount of incident 300K background radiation in wavelength region shorter than 30 μm is found negligibly small (ca. 0.4 % of the incident QCL power per pixel).

Thus, observations made with the transmission-type THz microscope are not influenced by infrared radiation from 300K environment.

Table 3. Comparison of incident QCL power per pixel with incident 300K background radiation per pixel
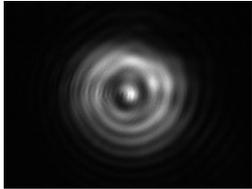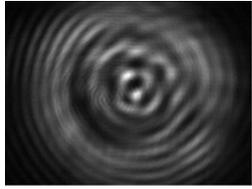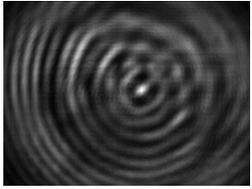
Radiation sources		Incident power per pixel	Comments
THz-QCL		ca. 3 nW	Illumination area : 5.64 mm in diameter. Seven Si lenses, filter and Si package window exist between QCL and THz-FPA. Atmospheric transmittance : 61 % (24 Celsius - 58 % relative humidity - 64 cm distance between QCL and THz-FPA)
300K background	λ >30 μm	ca. 1 nW	As to background radiation around sample, two Si lenses, filter and Si package window are considered.
	λ <30 μm	ca.13 pW	

Next, SNR values of the THz microscope were measured for a couple of different illumination areas (diameters : ca. 3.7, 6.4 and 8.2 mm). In the measurements, no samples were put and QCL was operated at 60K (time-average power 0.54 mW). The results are shown in table 4. Analyses were carried out as follows; Using THz image obtained for illumination area of ca. 3.7 mm in diameter, background level is calculated for the outside of the illumination area and is subtracted from 320x240 whole area so that total signal value is obtained by integrating signal of each pixel over the

whole area. This total signal value is taken as the signal of the illumination area and is divided by the number of pixels over the area. Thus, the average signal value per pixel is obtained and is divided by noise value (see the measured SNR).

The measured SNR value for the illumination area of 6.4 mm in diameter is compared with the predicted value shown in the previous paper (see Fig.13 in reference [9]). In the case of the illumination area of 5.64 mm in diameter, SNR value is calculated to be 550~880 from the reference. Considering differences in QCL power (or QCL operation temperature), illumination area and overall transmittance of optics as well as atmospheric transmittance between the calculations[9] and the measurements, this SNR value is converted to 59~94 which is consistent with the measured SNR value of ca. 70.

Table 4. THz images of the illumination areas without sample and values of SNR

Illumination areas	ca. 3.7 mm in diameter	ca. 6.4 mm	ca. 8.2 mm
THz images of illumination areas			
Measured SNRs	ca. 220	ca. 70	ca. 36
Calculated SNRs[*]	173~276	59~94	36~57

[*]) NEP value of THz-FPA itself is in the range of 25~40 pW[9].

3. THz IMAGERIES

Figures 8 (a), (b) and (c) show THz images of human hair (ca. 70 μm in diameter) put under a sheet of paper. Figure 8 (a) is a real-time image (frame rate 30 Hz), namely, no lock-in function, no frame integration, no spatial filter. In this case, SNR of hair detection is estimated to be ca. 3.4. Figures 8 (b) and 8 (c) are lock-in images taken with 16 frames integration, where the sync signal output of the THz camera was applied to control switching QCL on/off at lock-in frequency of 3.75 Hz. In Fig.8 (b), SNR of hair detection is ca. 16. Figure 8 (c) was taken with 3x3 spatial filter which improved SNR up to 47. It can be seen in all cases that THz camera can resolve human hair, namely, the camera has a high spatial resolution, and the lock-in function proves very powerful to improve overall performance of THz camera.

A couple of concentric interference patterns appear in Fig.8, which is due to strong coherency of QCL. To reduce these patterns, the THz images of human hair put under a sheet of paper were divided by the corresponding THz images of the same sheet of paper, so that Figs. 8 (d), (e) and (f) were obtained.

Figures 9 (a) and (b) show THz images of tablet put inside envelope and metallic clip put under flours, respectively. Length of long side in THz image is 7.5 mm because the microscopic optics has the magnification ratio of 1, as described in table 1. The lock-in imaging function as well as frame integration and spatial filter were applied (lock-in frequency 3.75 Hz) to increase SNR. Tablet and clip are clearly seen.

Figures 10 (a), (b) and (c) show sample setup, THz images prior to and during flowing ethanol and water, respectively. Both liquids flowed inside 125 μm thick PVDF (Polyvinylidene difluoride) membranes due to capillary effect. Neither lock-in function nor integration function were applied to the experiments (frame rate 30 Hz). It is seen in Fig. 10 (c) that ethanol (upper) is much more transparent than water (lower).
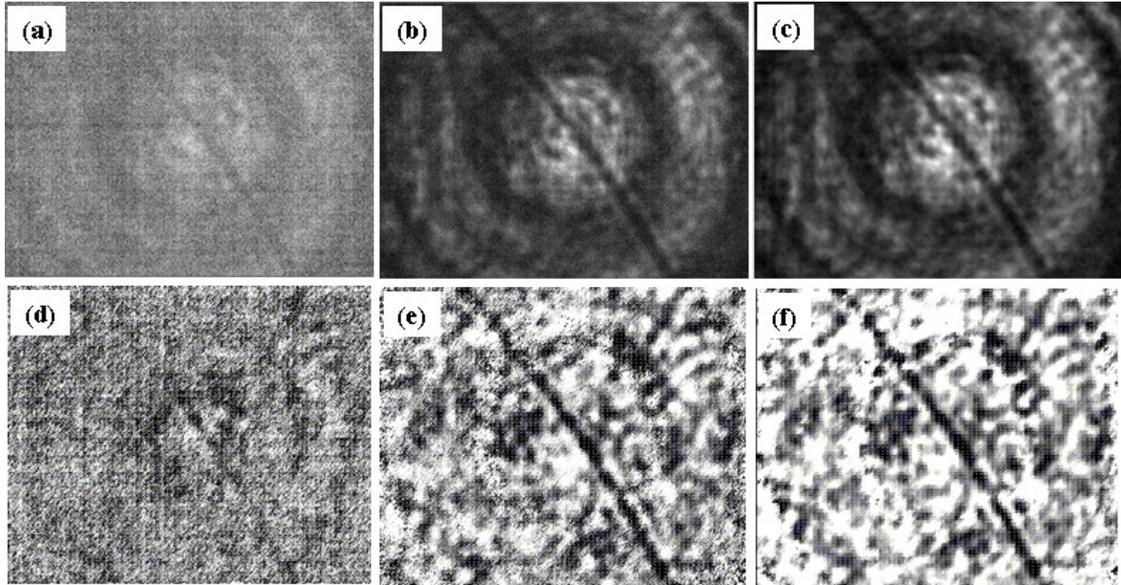

Fig.8 THz images of human hair put under a sheet of paper. (a) Real-time image (no lock-in function, no frame integration, no spatial filter : SNR~3.4), (b) Lock-in image (lock-in frequency 3.75Hz, 16 frames integration, no spatial filter : SNR~16), (c) Lock-in image (lock-in frequency 3.75Hz, 16 frames integration, 3x3 spatial filter : SNR~47). Images shown in (d), (e) and (f) were obtained with the procedure described in the text.
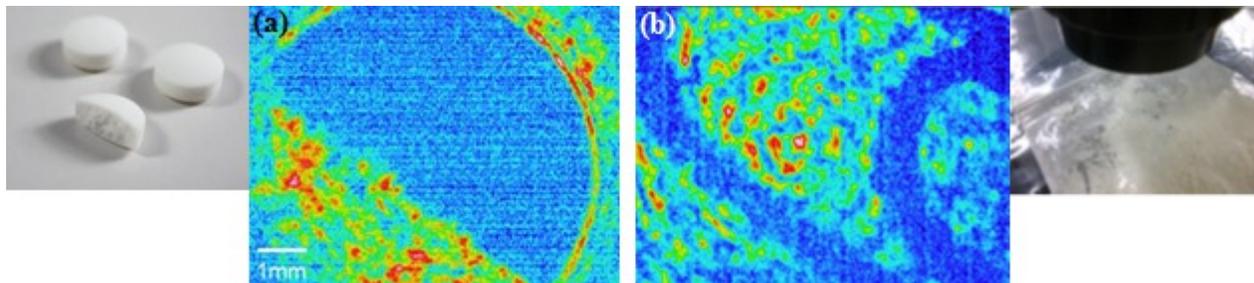

Fig.9 (a) Visible picture of tablet (left) and THz image of tablet put inside envelope (right) [frame integration: 2, spatial filter: 4x4] and (b) THz image of metallic clip put under flours (left) and visible picture of sample (right) [frame integration: 4, spatial filter: 2x2]. Both images were taken with lock-in imaging function (lock-in frequency 3.75 Hz).
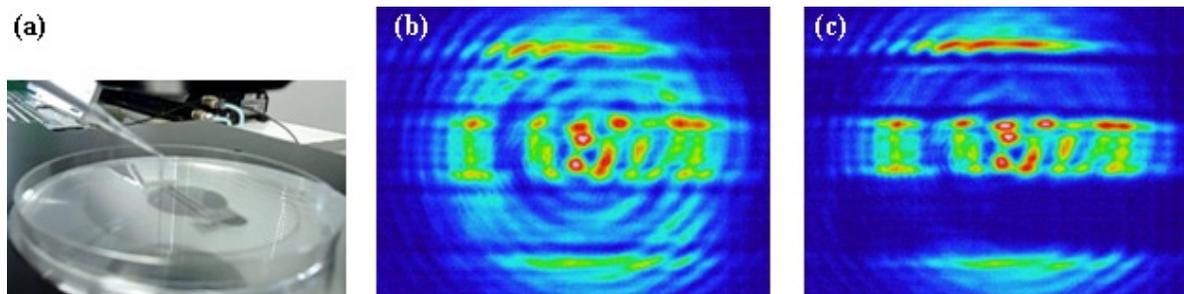
Fig.10 (a) Sample setup, (b) THz image prior to flowing ethanol and water, (c) THz image during flowing ethanol (upper) and water (lower).

6. SUMMARY

Real-time transmission-type THz microscope was developed, which is composed of QCL (emission line at 2.83 THz), real-time THz camera and illumination optics. The performances of the THz microscope were analyzed and measured. The measured performance, such as SNR at the sample plane, is found consistent with the calculation, using the measured values on time-average power of QCL, transmittance of the optics, atmospheric transmittance and NEP values of THz-FPA itself. The THz microscope has lock-in imaging function as well as integration functions such as frame integration and spatial filter. These functions are found very efficient in improving SNR values. Especially, the lock-in function is very powerful. Finally, THz images obtained with the THz microscope are presented, which show that the THz microscope certainly plays an important role in observing biomedical samples.

ACKNOWLEDGEMENTS

REFERENCES

[1] Ogawa, Y., Hayashi, S., Oikawa, M., Otani, C., and Kawase, K., "Interference terahertz label-free imaging for protein detection on a membrane," OPTICS EXPRESS, **16**, pp.22083-22089 (2008).

[2] Brun, M-A., Formanek, F., Yasuda, A., Sekine, M., Ando, N., and Eishii, Y., "Terahertz imaging applied to cancer diagnosis," Phys. Med. Biol., **55**, pp.4615-4623 (2010) .

[3] Minamide, H., and Ito, H., "Frequency-agile terahertz-wave sources and applications to sensitive diagnosis of semiconductor wafers," Proc. SPIE, **8023**, 802301 (2011).

[4] Kawase, K., "Terahertz imaging for drug detection and large-scale integrated circuit inspection," Optics & Photonics News, **15**, pp.34-39 (2004).

[5] Hosako, I., Sekine, N., Oda, N., Sano, M., Kurashina, S., Miyoshi, M., Sonoda, K., Yoneyama, H., and Sasaki, T., "A real-time terahertz imaging system consisting of terahertz quantum cascade laser and uncooled microbolometer array

detector," Proc. SPIE, **8023**, 80230A (2011).

[6] Taday, P. F., Bradley, I. V., Arnone, D. D., and Pepper, M., "Using Terahertz Pulse Spectroscopy to Study the Crystalline Structure of a Drug: A Case Study of the Polymorphs of Ranitidine Hydrochloride," J. Pharmaceutical Sci., **92**, pp.831-838 (2003).

[7] Fitzgerald, A. J., Cole, B. E., and Taday, P. F., "Nondestructive Analysis of Tablet Coating Thicknesses Using Terahertz Pulsed Imaging," J. Pharmaceutical Sci., **94**, pp.177-183 (2005).

[8] Shen,Y. C., Taday, P. F., Newnham, D. A., and Pepper, M., "Chemical mapping using reflection terahertz pulsed imaging," Semicond. Sci. Technol. **20**, pp.S254–S257 (2005).

[9] Oda, N., Lee, A. W. M., Ishi. T., Hosako, I., and Hu, Q., "Proposal for Real-Time Terahertz Imaging System, with Palm-size Terahertz Camera and Compact Quantum Cascade Laser," Proc. SPIE, **8363**, 83630A (2012).

[10] Williams, B. S., Kumar, S., Hu, Q., and Reno, J. L., "High-power terahertz quantum-cascade lasers," Electron. Lett., **42**, pp.89–90 (2006).

[11] Oda, N., "Uncooled bolometer-type Terahertz focal plane array and camera for real-time imaging," Comptes Rendus Physique, **11**, pp.496-509 (2010).